Photoemission studies of CdTe(100) and the Ag-CdTe(100) interface: Surface structure, growth behavior, Schottky barrier, and surface photovoltage

P. John, T. Miller, T. C. Hsieh, A. P. Shapiro, A. L. Wachs, and T. -C. Chiang
Department of Physics and Materials Research Laboratory, University of Illinois at Urbana-Champaign, Urbana, Illinois 61801
(Received 23 June 1986)

The clean CdTe(100) surface prepared by sputtering and annealing was studied with high-energy electron diffraction (HEED) and photoemission. HEED showed the surface to be a one-domain, (2×1) reconstruction. Photoemission spectra showed two surface-shifted components for the Cd $4d$ core level, with an intensity ratio of about 1:3, accounting for nearly an entire atomic layer. No surface-induced shifts for the Te $4d$ core level were detected. A model is proposed for the surface structure in which the surface layer is free of Te, and Cd atoms form dimers resulting in a (2×1) reconstruction; in addition, about $\frac{1}{4}$ of the surface area is covered by excess loosely attached Cd atoms. Ag was evaporated on the surface at room temperature and found to grow three dimensionally in the [111] direction. The Ag was found to interact only weakly with the substrate, although the Cd atoms originally loosely bound on top of the surface were found to float on the evaporated Ag islands. A small coverage-dependent surface photovoltage, induced by the synchrotron radiation used for photoemission, was observed; with this effect taken into account, band bending was monitored, the final Fermi-level position being near 0.96 eV above the valence-band maximum. This corresponds to a Schottky-barrier height of about 0.60 eV for the n-type sample used in this experiment. The mechanism for generation of the surface photovoltage will be discussed.

I. INTRODUCTION

Characterization of semiconductor surfaces and metal overlayers on these surfaces has been the focus of much work in recent years. Surface atoms generally exhibit different properties than bulk atoms. In semiconductors, the surface atoms often relax or reconstruct into geometries that are perturbed from the bulk crystal structure. Also, since surface atoms are not in the same chemical environment as the bulk atoms, there are usually observable shifts in the core-level binding energies of electrons. Surface core-level shifts and different surface reconstructions have been correlated in several cases.[1–6]

Metal overlayers evaporated onto a semiconductor surface may exhibit many different types of growth behaviors depending on the system and the growth condition. Commonly observed phenomena associated with film growth include intermixing, segregation, clustering, chemical reaction, etc.; and the growth mode can be three-dimensional, two-dimensional, or two-dimensional initially followed by three-dimensional growth. With high-resolution core-level photoemission studies, atoms in different atomic environments can often be distinguished by their different core-level binding energies, thus allowing distinction of these different possible growth behaviors.[7]

Most of the previous work has centered on the elemental semiconductors, Si and Ge, and on certain III-V compound semiconductors such as GaAs. This study is of the (100) surface of the II-VI compound semiconductor CdTe with Ag as the metal overlayers. In compound semiconductors, the actual surface composition is a question. High-energy electron diffraction (HEED) showed the clean CdTe(100) surface to be a one-domain, (2×1) reconstruction. Photoemission spectra showed two surface-shifted components for the Cd $4d$ core level, with an intensity ratio of about 1:3, accounting for nearly an entire atomic layer. No surface-induced shifts for the Te $4d$ core level were detected. A model is proposed for the surface structure in which the surface layer is free of Te, and Cd atoms form dimers resulting in a one-domain (2×1) reconstruction; in addition, Cd atoms equivalent to about $\frac{1}{4}$ monolayer are loosely bound on top of the surface. Thus, two kinds of surface Cd atoms exist, one kind (the majority) bound to Te and the other kind (the minority) bound to Cd (like, for example, in antisite defects) resulting in two surfaces shifts with opposite signs.

Ag was evaporated on the surface at room temperature and found to grow three dimensionally in the (111) direction. Based on the measured core-level line shapes and energy positions, the Ag was found to interact only weakly with the substrate, although the Cd atoms originally loosely bound on top of the surface were found to float on the evaporated Ag islands.

The Ag overlayer showed a well-developed Fermi edge in the photoemission spectra for Ag coverages over about one half of a monolayer. This edge was observed to have a higher kinetic energy than the edge derived from a Au foil in electrical contact with the sample back, indicating the presence of a surface photovoltage induced by the synchrotron radiation used for photoemission.[8–11] With this effect taken into account, band bending was monitored by determining the shifts in bulk core-level energies, the final Fermi-level position being near 0.96 eV above the valence-band maximum (VBM) of CdTe. For our n-type sample, this corresponds to a Shottky-barrier height of

about 0.60 eV.

With an n-type substrate, one would normally expect a surface photovoltage of opposite polarity to that observed in this experiment. Moreover, the light intensity used in this experiment was rather weak, and the observation of a surface photovoltage at room temperature is rather unusual.[8-11] The mechanism leading to the generation of this surface photovoltage will be discussed.

II. EXPERIMENTAL DETAILS

Angle-integrated photoemission spectroscopy was used to determine the Cd 4d and Te 4d core-level binding energies and line shapes of the CdTe(100) surface. The experiment was conducted at the Synchrotron Radiation Center of the University of Wisconsin—Madison. The Grasshopper Mark V monochromator was used to select photon energies. A cylindrical mirror analyzer was used to analyze emitted electron kinetic energies. Since the photoelectron escape depth depends on the kinetic energy, the degree of surface sensitivity can be varied by choosing different photon energies. Photon energies of 32 and 52 eV were selected for Cd 4d bulk- and surface-sensitive spectra, respectively. For Te 4d bulk- and surface-sensitive spectra, photon energies of 52 and 80 eV were used. The total instrumental energy resolution was approximately 0.3 eV as determined from the measured widths of the Fermi edges of a Au foil in electrical contact with the sample back. Fermi-level positions for this Au foil as well as those for the Ag films on the CdTe substrate were determined by photoemission from the valence bands.

The n-type CdTe(100) sample was In doped with a resistivity of $2\times10^{+8}$ Ω cm. It was aligned to within one-half degree with Laue x-ray scattering, and then mechanically polished in this orientation using 0.3 μ alumina. The sample was then mechanochemically polished with a 0.2% bromine-in-methanol solution so that the surface was free of visible defects. Several cycles of sputtering with 500-eV Ar^+ ions and annealing at 400 °C were necessary to obtain a clean, ordered surface. The surface structure was examined using high-energy electron diffraction. The sample was found to have a sharp one-domain (2×1) reconstructed diffraction pattern. Auger spectra showed no contamination above our detection limit (about 1 at. %).

Ag was evaporated from a tungsten crucible; the evaporation temperature was reached via electron-beam heating. During evaporation, the substrate was kept at room temperature. Film thicknesses were determined by calibrating the evaporation rate with a quartz-crystal monitor and then opening the shutter for the necessary amount of time. High-energy electron diffraction showed the Ag to grow in a highly three-dimensional manner with the Ag [111] direction oriented with the CdTe(100) sample normal. The Ag clusters grew in two domains such that the Ag [110] direction was in either the CdTe [010] or [001] direction. Photoemission spectra were recorded for Ag coverages of 0.5, 1, 2, 5, and 10 monolayers. One monolayer is defined here as the amount of Ag necessary to form 1 atomic layer in Ag(111).

III. RESULTS

A. Surface core-level shifts and structure for CdTe(100)-(2×1)

Figure 1 shows the bulk- and surface-sensitive Cd 4d core-level spectra (dots) for the clean CdTe(100)-(2×1) surface. The binding energy is referred to the Fermi level of a Au foil in electrical contact with the sample back. Clearly, there is additional structure on both the higher and lower binding-energy sides of the main spin-orbit split peak. This additional structure is relatively more intense in the surface-sensitive case, indicating the presence of at least two separate surface shifts in the core level. These core-level line shapes were analyzed by fitting the data with a Voigt function (Gaussian function convolved with Lorentzian function) for each spin-orbit component of the main peak and surface-shifted peaks; the background function was assumed to be a smooth cubic polynomial. The discussion of this fitting procedure can be found in previous publications,[4-7,12] and will not be repeated in detail here. The initial assumption made is that each shifted component has a line shape that is identical to the main component, only differing in intensity and position. This assumption was insufficient in fitting the surface component that is shifted to lower binding energy due to additional broadness of this feature. One possible reason for this broadening is that there is not one shift, but several closely spaced shifts appearing as one smeared shift due to inhomogeneous atomic environments. To approximately account for this broadening, we allowed the Gaussian width of this surface-shifted component to be larger than that of the other two components. The Cd bulk-sensitive ($h\nu=32$ eV) and surface-sensitive ($h\nu=52$ eV) spectra

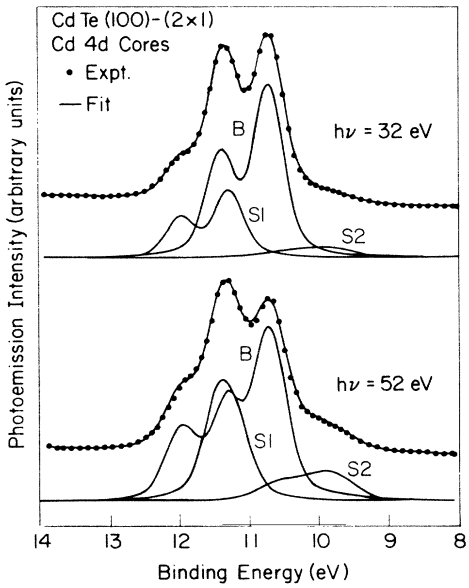

FIG. 1. Angle-integrated photoemission spectra (dots) of the Cd 4d core level for the clean CdTe(100)-(2×1) surface. The theoretical fits to the overall line shapes and the separate contributions from the bulk (B) and the two surface-shifted components ($S1$ and $S2$) are shown with the solid curves. Binding-energy scale is referenced to the Fermi level.

were fitted simultaneously with the Lorentzian width, spin-orbit splitting, and surface shifts constrained to be the same for both spectra. The results of the fit and the separate contributions from the bulk (B) and the two surface components ($S1$ and $S2$) are shown in Fig. 1 by the solid curves. Table I lists some pertinent fitting parameters. The surface-to-bulk (S/B) intensity ratios confirm that the shifted components are indeed surface features. The ratio of intensities, $S1/S2$, should be the same for surface and bulk spectra; the small deviation we obtain is due to the uncertainty in measuring the low intensity of the $S2$ component of the bulk-sensitive spectra (see Fig. 1). The slight difference in the Gaussian widths for surface and bulk spectra is attributed to the change in photon energy and therefore photon energy resolution. The quality of the fit is very good, although some small differences are visible due to the approximations associated with the fitting assumptions.

Figure 2 shows the bulk- and surface-sensitive Te $4d$ core-level spectra (dots) for the clean surface. No surface-shifted component is visibly apparent in the data and our fitting routine also gave no indication of the existence of a shift in the Te $4d$ core-level binding energy. Again, the two spectra shown in Fig. 2 were fitted simultaneously with the same constraints as were used for the Cd $4d$ spectra. No surface-shifted peak is used in fits (solid curves) shown in Fig. 2. Fitting parameters are shown in Table II. The branching ratios for bulk and surface spectra vary due to final-state effects.[4]

From the intensity ratios of surface and bulk contributions, an analysis can be made of the fraction f of the surface covered by atoms with surface-shifted core-level binding energies.[12] Let I_1 be the emission intensity of each (100) atomic layer of Cd. Then the contribution of surface shifted-atoms I_S is

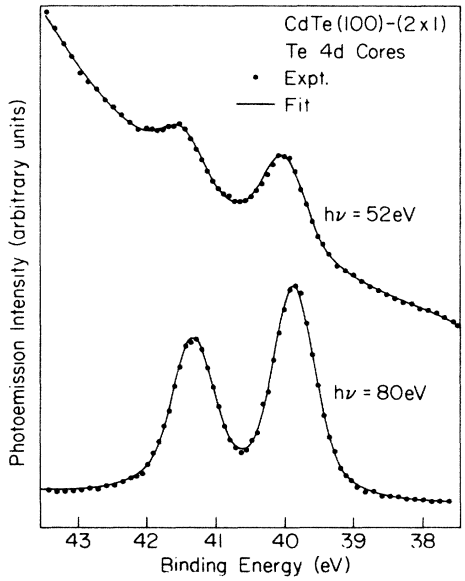

FIG. 2. Angle-integrated photoemission spectra (dots) of the Te $4d$ core level for the clean CdTe(100)-(2×1) surface. The theoretical fits are shown with the solid-line curves. No surface-shifted component was observed.

$$I_S = fI_1 \ . \tag{1}$$

The bulk contribution I_B is then

$$I_B = (1-f)I_1 + I_1 e^{-d/L} + I_1 e^{-2d/L} + \cdots \ , \tag{2}$$

where $d = 3.24$ Å is the spacing of consecutive planes of Cd atoms and L is the electron escape length for CdTe. Solving these two equations for f yields

$$f = 1/[(1+I_B/I_S)(1-e^{-d/L})] \ . \tag{3}$$

The ratio I_B/I_S from the result shown in Table I was 1.18 for the surface-sensitive Cd core-level spectrum; here, I_S is taken to be the sum of the intensities of $S1$ and $S2$. The value of L was estimated from the universal curve[13] and from earlier studies of GaAs and Ge to be in the range 5.0–5.5 Å.[4,12,14–17] From these values, we obtain $f = 0.96$–1.03 indicating that the surface layer is composed almost entirely of Cd surface-shifted atoms. Assuming that $f = 1$, the atoms shifted by 0.571 eV to higher

TABLE I. Results of nonlinear least-squares fit of the Cd $4d$ core-level line shape for the clean CdTe(100)-(2×1) surface. The branching ratio is the intensity ratio between the $4d_{3/2}$ and $4d_{5/2}$ spin-orbit-split components. The S/B intensity ratio is the ratio between the surface and the bulk contributions. The binding energy of the bulk component (B) of the Cd $4d_{5/2}$ core is 10.72 eV referred to the Fermi level.

	Surface sensitive $h\nu = 52$ eV	Bulk sensitive $h\nu = 32$ eV
Spin-orbit splitting (eV)	0.694	0.694
Branching ratio	0.658	0.587
Surface shift (eV)		
$S1$	0.571	0.571
$S2$	−0.863	−0.863
Gaussian width (eV)		
B	0.444	0.383
$S1$	0.444	0.383
$S2$	0.680	0.783
Lorentzian width (eV)	0.212	0.212
S/B intensity ratio		
$S1$	0.633	0.388
$S2$	0.218	0.090

TABLE II. Results of nonlinear least-squares fit of the Te $4d$ core-level line shape for the clean CdTe(100)-(2×1) surface. The branching ratio is the intensity ratio between the $4d_{3/2}$ and $4d_{5/2}$ spin-orbit-split components. The binding energy of the $4d_{5/2}$ core is 39.86 eV referred to the Fermi level. No surface shifts were observed.

	Surface sensitive $h\nu = 80$ eV	Bulk sensitive $h\nu = 52$ eV
Spin-orbit splitting (eV)	1.469	1.469
Branching ratio	0.732	0.552
Gaussian width (eV)	0.562	0.580
Lorentzian width (eV)	0.296	0.296

binding energy (type $S1$) account for 74% of the surface layer, while those atoms shifted by 0.863 eV to lower binding energy (type $S2$) make up the remaining 26%.

In light of these core-level line shapes, the surface (2×1) reconstruction can be explained by a model in which the surface atoms form dimers, similar to Ge(100) and Si(100).[18,19] A vacancy model, for example, cannot explain the observed intensity of the surface-shifted Cd core level.[4] Ge(100) and Si(100) have (2×1) reconstructed surfaces, but both have two domains 90° apart, whereas CdTe(100) has only one domain. In the (100) diamond structure (Si and Ge), adjacent planes are rotated by 90°. Due to the presence of random atomic-step defects on the Ge and Si surfaces, both domains are observed with equal probability. In the (100) zinc-blende structure (CdTe), adjacent planes are also rotated by 90°, but they are, in addition, composed of different materials. Consecutive planes of the same element are identical. Thus the CdTe(100) surface can be either Cd- or Te-terminated.[20] A complete absence of either Cd or Te on the surface would result in any steplike defects on the surface being actually an even number of planes, and each step surface would have the same orientation as every other one. There is a relatively intense Cd $4d$ surface-shifted core-level component, and there is not one for the Te $4d$. This implies that the CdTe(100)-(2×1) surface is Cd terminated (i.e., the surface layer is void of Te). So, in this model, the CdTe(100) would show only a single-domain (2×1) reconstruction instead of the two domains observed in Ge(100) and Si(100); this is consistent with the experimental observation.

The absence of Te on the surface is likely a result of the sample preparation procedure (sputtering followed by annealing). Te is much more volatile than Cd, and annealing the surface, necessary to restore surface order, inevitably drives away Te. A similar phenomenon is well known in the preparation of III-V compound semiconductor surfaces.[20,21] In those systems, the surface can often be made to be terminated entirely by the group-III element by annealing. To obtain surfaces with richer group-V compositions, molecular-beam-epitaxy techniques are needed in which the sample surface is bombarded by a group-V molecular beam. It is also commonly observed in the case of III-V compounds that the group-III-terminated surface has excess group-III element after sputtering and annealing. This seems to be also the case for CdTe(100). The excess elemental Cd gives rise to the $S2$ component, with a binding energy characteristically shifted to a smaller value relative to the bulk contribution.[22] From our intensity analysis discussed above, about $\frac{1}{4}$ of the surface is covered by this excess elemental Cd. The remaining $\frac{3}{4}$ of the surface area is not affected, exhibiting a Cd core surface shifted to higher binding energies ($S1$).

As will be shown below, the excess elemental Cd on the surface giving rise to the $S2$ component can be lifted from the surface when Ag is deposited. These Cd atoms simply segregate on top of the Ag film. Below the Ag overlayers, the CdTe substrate becomes nearly perfectly terminated by Cd, with the new $S1$-to-B component intensity ratio corresponding to a full monolayer. A similar behavior has been recently reported for the system of Ag deposited on Ge(111)-$c(2\times8)$, in which surface Ge atoms, originally loosely attached to the substrate ("adatoms"), become segregated on top of the Ag overlayer.[6]

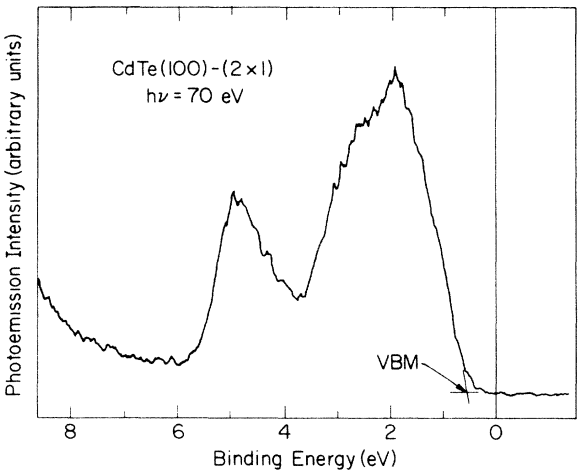

FIG. 3. Angle-integrated photoemission spectra of the clean CdTe(100)-(2×1) surface in the valence-band region using a photon energy of 70 eV. Binding-energy scale is referenced to the Fermi level. The position of the valence-band maximum (VBM) is indicated.

B. Valence-band maximum

Figure 3 shows an angle-integrated photoemission spectrum of the valence-band region for clean CdTe(100) taken with a photon energy of 70 eV. At this photon energy, the spectrum should resemble the valence density of states.[21] The binding-energy scale is referred to the Fermi level of the Au foil in contact with the sample back. The spectrum is terminated at about 8 eV binding energy, that is, before the onset of the strong Cd $4d$ core-level emission. The energy position of the VBM, which will be important for the determination of the Schottky-barrier height, is determined by locating the leading edge of the spectrum on the low binding-energy side, as indicated in Fig. 3 by the crossing point of the two straight-line segments. The VBM is at 0.59 eV below the Fermi level. The binding energy of the bulk Cd $4d_{5/2}$ core level is 10.13 eV referred to the VBM, determined by measuring the energy spacing in the spectrum.

At high Ag coverages, emission from near the VBM of CdTe becomes masked by the strong emission from Ag. The position of the VBM near the surface region is then indirectly determined by measuring the position of the bulk Cd core level.

C. Surface Fermi levels and photovoltages for Ag-covered CdTe(100)

For Ag coverages beyond 0.5 ML, a well-developed Fermi edge is observed in the photoemission spectra since the Ag growth is highly three-dimensional and rather large Ag islands are formed on the surface.[4,15,16] The Fermi edge of the Ag islands is at higher kinetic energies

than that of the Au foil in electrical contact with the sample back. This is a clear indication of a surface photovoltage (SPV).[8–11] Sample charging effects can be ruled out for two reasons. Generally, charging effects exhibit time-dependent behavior and none was observed here. Moreover, the sign of the voltage is opposite to what would be expected for both the time-dependent and steady-state cases. Since the chamber was darkened during experiments, the only possible light source able to induce a SPV was the synchrotron radiation used for measuring the photoemission spectra. The observed SPV was found to be independent of the photon energy used (32—80 eV) and of the intensity of the synchrotron light (which was varied by a factor of 2 with no effect upon the SPV).

The SPV, which equals the change in band bending induced by light, is plotted in Fig. 4 as a function of Ag coverage. This voltage increases in magnitude for increasing Ag coverages, and by extrapolation, is zero for zero Ag coverage. At zero Ag coverage, there is no surface Fermi edge in the photoemission spectra, disallowing a direct comparison between the bulk and surface Fermi levels. Experimentally, we did not observe evidence for any measurable SPV for the clean CdTe(100) surface; that is, we have taken two spectra with very different incident synchrotron-radiation light intensities and observed no relative shifts within our experimental errors. It has been demonstrated that pure semiconductor surfaces such as GaAs and CdS (which are very similar to CdTe) at room temperature would require much higher light intensities to produce any noticeable SPV.[8–11]

Clearly, the SPV observed here is induced by the presence of Ag. The usual mechanism of SPV is the generation of electron-hole pairs within the semiconductor, with one type of charge carrier (holes for n-type samples) driven toward the surface by the band bending and trapped there. This mechanism would reduce the amount of surface band bending, contrary to what is observed experimentally for the present system. In any case, the recombination process within the semiconductor is fairly efficient at room temperature, disallowing any significant net carrier transport to occur; thus, no measurable SPV resulting from this mechanism is expected under our experimental conditions. These observations point to a different mechanism. This will be discussed further after the core-level spectra are examined.

D. Core-level spectra for Ag-covered CdTe(100)

Figures 5 and 6 show the Cd 4d and Te 4d surface-sensitive spectra for increasing Ag coverages. The binding-energy scale is referred to the Fermi level of the Au foil for the clean surface and to the Fermi level of the Ag overlayer for the Ag-covered surfaces. That is, the energy reference is the surface Fermi level (note that there is no SPV for the clean surface). With this local energy reference, band-bending effects associated with the SPV are removed.

The only clearly visible change to the Te 4d spectra for increasing Ag coverages is an energy shift between the clean case and the Ag-covered cases. The energy shift is due to a band bending induced by Ag adsorption.[9,15] The Cd 4d core-level spectra show the same shift; in addition, the $S2$ component moves closer to the B component for increasing Ag coverage.

All spectra shown in Figs. 5 and 6 were fitted to theoretical curves via methods similar to those used for the clean spectra discussed above. For the Te 4d core, the Lorentzian width was constrained to be the value obtained in the fit of the clean spectra; all the other fitting parameters were allowed to vary. Except for the Gaussian width which increases slightly for higher Ag coverages (by 0.02 eV) and the shift due to band bending noted above, all line-shape fitting parameters came out to be the same as the clean case within close tolerances. The lack of chemi-

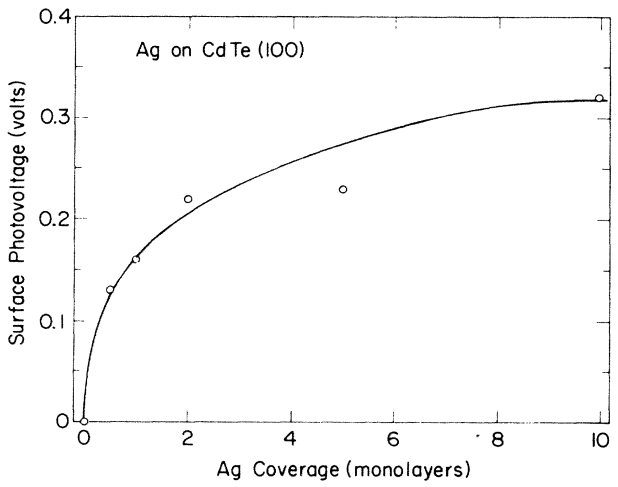

FIG. 4. The measured surface photovoltage (SPV) as a function of Ag coverage. The circles are data points. The smooth curve is just a guide to the eye.

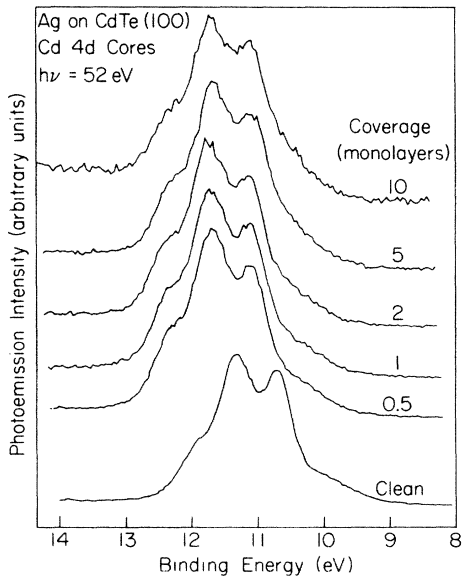

FIG. 5. Angle-integrated photoemission spectra of the Cd 4d core level for increasing Ag coverages taken with a photon energy of 52 eV. Binding-energy scale is referenced to the surface Fermi level.

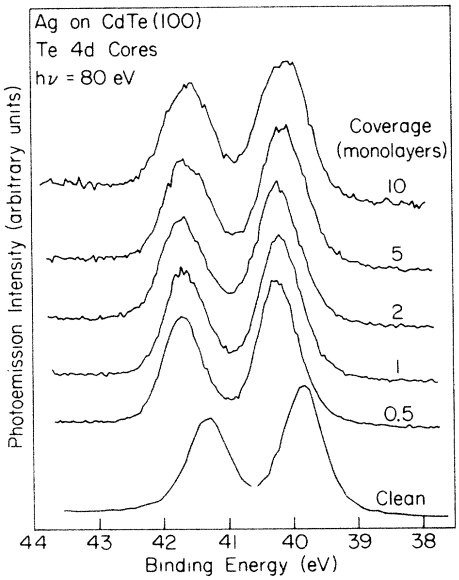

FIG. 6. Angle-integrated photoemission spectra of the Te $4d$ core level for increasing Ag coverages taken with a photon energy of 80 eV. Binding-energy scale is referenced to the Fermi level.

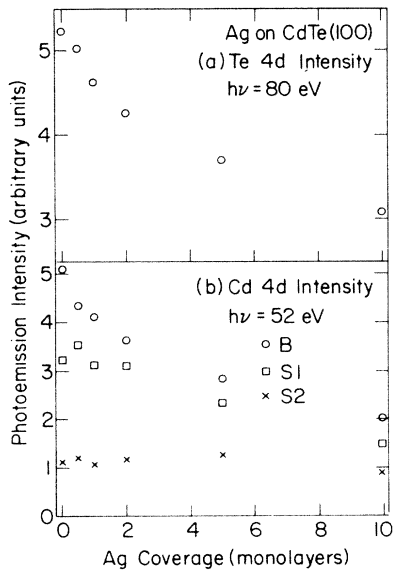

FIG. 7. (a) Relative photoemission intensities (normalized peak areas) for the Te $4d$ core level for increasing Ag coverages. (b) Relative photoemission intensities for the B, $S1$, and $S2$ contributions of the Cd $4d$ core level for increasing Ag coverages.

cally shifted component indicates that the surface is not disrupted by Ag. The Cd $4d$ spectra were fitted similarly. The results show the same band-bending shift and a similar small broadening as for the Te spectra. The $S2$ component moves closer to the B component for higher Ag coverages, as noted above, but the energy separation between the B and $S1$ components remains constant. The slight increase in Gaussian width for both the Cd and Te core levels is likely a result of inhomogeneous broadening associated with Ag-island formation.

The relative core-level photoemission intensities have been determined for the Cd and Te $4d$ core levels. The results are shown in Fig. 7. The intensity measurements are somewhat uncertain due to experimental errors such as uncertainties in the synchrotron source intensity used for normalization. The spectra for higher Ag coverages are noisier due to a reduced photoemission intensity leading to a larger uncertainty. Figure 7(a) shows the relative intensity of the Te $4d$ core level as a function of Ag coverage. The shape of the curve is consistent with the highly three-dimensional Ag growth on the surface that is implied by the HEED patterns. If the overlayer were perfectly smooth, the core-level intensity at 10 ML Ag coverage would be about $\frac{1}{50}$ of the experimentally observed value.

Figure 7(b) shows the relative intensities of the B, $S1$, and $S2$ components of the Cd $4d$ core level as a function of Ag coverage. The intensity of the $S2$ component stays relatively constant for all coverages, while the other two components decrease in a fashion similar to the Te $4d$. The fact that the $S2$ component intensity remains constant indicates that the Cd atoms giving rise to the $S2$ component are floating to the top of the Ag after it is deposited on the surface. Also, the intensity of the $S1$ component increases going from the clean surface of 0.5 monolayer of Ag coverage, while the main component undergoes a sharp decrease in the same interval. In other words, the intensity ratio between the $S1$ and B components increases significantly. Equation (3) was used to determine the fraction f of the CdTe surface monolayer composed of $S1$-type Cd atoms for the 0.5-monolayer Ag coverage. The assumption is made that $S2$-type Cd atoms are floating on the Ag, so that they are no longer on the CdTe surface monolayer. For values of $L = 5.0$–5.5 Å, we found f to be between 0.94 and 1.01; about the entire CdTe surface is now composed of $S1$-type Cd. To explain this phenomenon, the following model is proposed. Sputtering followed by annealing removes all Te from the surface, resulting in a surface terminated by dimerized Cd ($S1$ type) with some excess scattered Cd (type $S2$) atoms on top of other Cd atoms, the Te normally in between missing. The Cd atoms lying immediately under these $S2$ Cd atoms exhibit binding energies that are not measurably shifted from the bulk binding energy. After evaporation of Ag, the $S2$ Cd atoms float on top of the Ag, leaving the bulk-type atoms underneath to transform into $S1$ Cd atoms. The fact that Ag forms highly three-dimensional islands on the surface and that there is no clearly discernible chemical shifts indicates that the interaction between Ag and CdTe is extremely weak. Evidently, the presence of Ag on the surface does not affect the energy separation between the $S1$ and B components. A similar behavior has been observed for Ag deposited on Ge(111) and Ge(100).[4,6]

Figure 8 shows the binding energy of the $S2$ component of the Cd $4d_{5/2}$ core level relative to the Fermi level of the Ag islands. It shifts as a function of the Ag coverage due to size effects, as the Ag-island size increases for higher coverages (verified by HEED). The shift in core-level binding energies of inhomogeneous systems is a com-

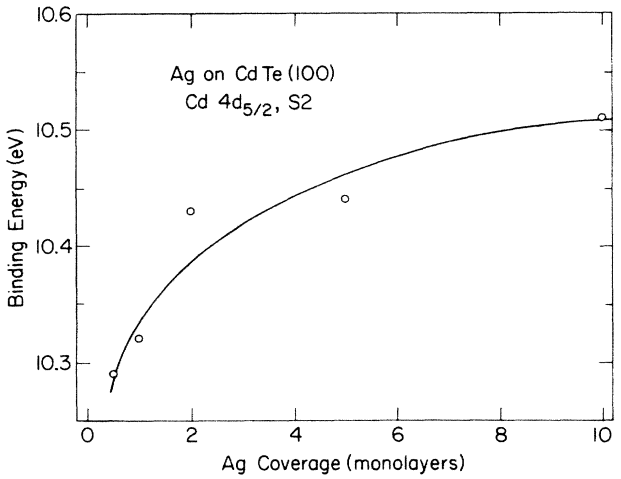

FIG. 8. Binding energy of the Cd $4d_{5/2}$ of the $S2$ component referenced to the Ag Fermi level for increasing Ag coverages. Data points are indicated by circles. The smooth curve is just a guide to the eye.

plicated matter; it could be related to changes in electronegativity, electronic configuration, charge transfer, relaxation energy, etc.[7,23–27] We do not attempt to explain the observed shifts here. However, we do notice the similar trends in the data shown in Figs. 5 and 8. This may be a fortuitous coincidence or an indication of the dominance of a simple effect causing the shift; no speculations will be given.

E. Schottky-barrier height

From the results of deconvolution of the Cd $4d$ core-level line shape, the bulk Cd core-level binding energy is obtained relative to the local (surface) Fermi level. Since the VBM is determined to be at 10.13 eV above the bulk Cd $4d_{5/2}$ core level, we can determine the Fermi-level position relative to the VBM and the conduction-band minimum (CBM) at the surface. The results are shown in Fig. 9. The Fermi-level position relative to the band gap can also be deduced from the Te $4d$ core-level spectra which show no surface-induced shifts. The results agree with those deduced from the bulk Cd $4d$ core level within experimental uncertainties. At the lower Ag coverages for which the VBM was still experimentally visible, the results shown in Fig. 9 are also in excellent agreement with Fermi-level positions measured by the energy separation between the VBM and the Ag Fermi edge. Our results indicate that the Fermi-level position moves to about 0.96 eV above the VBM for Ag coverages greater than 0.5 ML. The band-gap energy of CdTe at room temperature is 1.56 eV.[28] For our n-type sample, this corresponds to a Schottky-barrier height of about 0.60 eV. This value is similar to the 0.66 eV for Ag on n-type cleaved CdTe(110) measured by a photoresponse technique.[29]

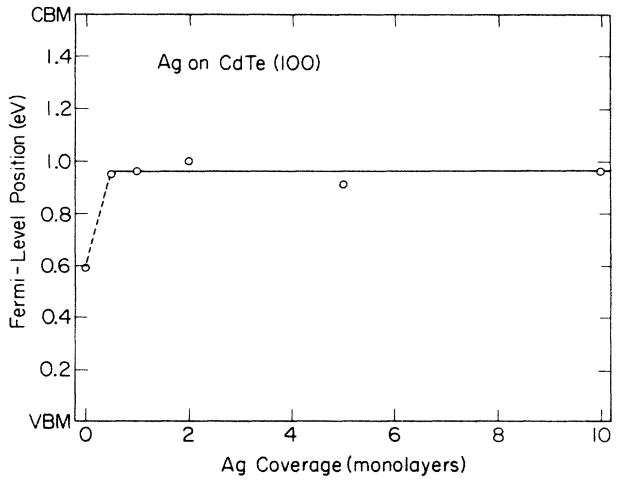

FIG. 9. Position of the Fermi level with respect to the band gap of CdTe near the surface for increasing Ag coverages. The energy zero is defined to be at the valence-band maximum (VBM). The conduction-band minimum (CBM) is at 1.56 eV at room temperature. The circles are data points. The solid line is the final pinning position, 0.96 eV above the VBM.

F. Mechanism for the surface photovoltage

For a detailed discussion of the SPV effects, the readers are referred to the excellent articles by Gatos and Lagowski[8] and by Brillson.[9]

Under very high-energy photon excitations, as in our experiment, electrons and holes with a wide spectrum of energies are generated in the sample. The net effect is always to reduce the "built-in" voltages in the system, because the carriers or charges diffuse or relax to "screen" the built-in voltages. Photovoltage inversion effects, as discussed by Gatos and Lagowsky, can occur only for specific low photon energies resonantly exciting particular electronic transitions.[8–11]

As already mentioned above, the band bending in the semiconductor itself, one of the built-in voltages in the system, can cause the separation of photon-generated charge carriers of different signs leading to a SPV. But the net transport of charge carriers within the semiconductor is effectively quenched at room temperature due to a rather high carrier recombination rate. In any case, any reduction in the upward band bending for our n-type sample resulting from the transport and accumulation of holes on the surface would lead to a SPV of the sign opposite to that actually observed. Thus, this mechanism, while important at low temperatures and/or high light intensities, is negligible for the present case.

From the result shown in Fig. 4, the SPV is clearly induced by the presence of Ag. This behavior strongly suggests that the built-in voltage responsible for the observed SPV is the potential difference between the Ag surface and the bare semiconductor surface. The authors speculate that the potential difference between Ag and CdTe is just the work-function difference, and that it becomes "screened out" by the light-induced charges resulting in a SPV. The net charge flow can be accomplished by, for example, a differential emission of low-energy secondary electrons associated with photoemission. The photoemission current from the sample is dominated by the very low-energy secondary electrons.

Unfortunately, we do not know the relevant numbers for the work functions. The relevant work function for CdTe(100) is the one for the ideal (2×1) Cd-terminated surface (without the excess Cd), a surface that we have not been able to prepare. The relevant work function for Ag is the one for the islands modified by the dielectric properties of the substrate.[15] All we can say is that the work function of the Ag islands decreases as a function of the island size.[15,30] Looking at the appropriate numbers for related systems such as CdS, CdSe, and Ag on GaAs, we believe that the work function of the Ag islands is smaller than the work function of CdTe(100).[9,11,15,30,31] Thus, without light and under equilibrium conditions the Ag surface is electrically positive relative to the CdTe surface. With light, the Ag islands collect some negative charges to compensate for the potential difference, resulting in an increase in band bending. This model explains the polarity of the observed SPV. Since the measured SPV does not change for different photon energies (32—80 eV) or different intensities (by a factor of 2), the potential difference between Ag and CdTe is completely bleached under our experimental conditions.

Since the Ag islands show negligible interaction with the substrate (for example, they do not even cause the energy separation between the $S1$ and B components of the Cd $4d$ core to change upon coverage), it is entirely plausible that the light-induced charges in Ag have a very long lifetime. Thus, while the clean semiconductor surface does not hold any appreciable amount of charge due to a fast recombination rate, the Ag islands can behave differently due to the weakness of the coupling between the Ag and the semiconductor.

The SPV increases as a function of Ag coverage. This behavior could be accounted for by two effects. The Ag grows in a highly three-dimensional fashion, and the CdTe surface is not fully covered by Ag at the highest Ag coverage in the present experiment. Because of this, the Ag islands increase in size as well as in number for increasing coverages. The increase in number simply increases the physical locations where charges can be stored. The increase in size reduces the work function of the Ag islands allowing more charge to be stored on each island. Both effects lead to a higher SPV as observed.

IV. SUMMARY

The clean surface of CdTe(100) prepared by sputtering and annealing has been investigated using high-energy electron diffraction and photoemission techniques. The surface was found to exhibit a one-domain (2×1) reconstruction. Two surface-shifted components, $S1$ and $S2$, were observed for the Cd $4d$ core level, with shifts of 0.57 eV to lower binding energy and 0.86 eV to higher binding energy, respectively. No surface shifts were observed for the Te $4d$ core level. The results were interpreted in terms of a Cd-terminated surface with the surface Cd atoms dimerized to form the (2×1) reconstruction. These dimerized surface Cd atoms corresponded to the $S1$ component. In addition, about $\frac{1}{4}$ of the surface was covered by excess elemental Cd as a result of the sample preparation procedure, giving rise to the weaker $S2$ component. The surface Ag layers were evaporated and a three-dimensional growth pattern was observed. The Ag overlayers were found to interact only weakly with the substrate. Only the $S2$ component of the Cd $4d$ core was observed to show a relative shift in binding energy with Ag coverage. From the measured photoemission intensities of the different core-level components, we concluded that the excess elemental Cd on the starting CdTe surface was floating on the Ag overlayer. A small SPV was observed, which increased for increasing Ag coverage, with a polarity corresponding to an increase in band bending. The result was interpreted in terms of the "flattening" of the built-in voltage between the Ag and CdTe. With the SPV taken into account, the energy positions of the local (surface) Fermi level and VBM were determined. The Fermi level was at 0.59 eV above the VBM for the clean surface, and shifted to near 0.96 eV above the VBM for Ag coverages above one-half monolayer. For our n-type sample, this gave a Schottky-barrier height of about 0.60 eV.

ACKNOWLEDGMENTS

This material is based upon work supported by the U.S. Department of Energy (Division of Materials Sciences), under Contract No. DE-AC02-76ER01198. Some of the equipment used for this research was obtained through grants from the National Science Foundation (Grant No. DMR-83-52083), the IBM Thomas J. Watson Research Center (Yorktown Heights, N.Y.), and the E. I. du Pont de Nemours & Company (Wilmington, DE). The Synchrotron Radiation Center (Stoughton, WI) of the University of Wisconsin—Madison is supported by the National Science Foundation under Contract No. DMR-80-20164. We acknowledge the use of central facilities of the Materials Research Laboratory of the University of Illinois, which is supported by the U.S. Department of Energy (Division of Materials Sciences), under Contract No. DE-AC02-76ER01198, and by the National Science Foundation under Contract No. DMR-80-20250.

[1]F. J. Himpsel, P. Heimann, T.-C. Chiang, and D. E. Eastman, Phys. Rev. Lett. **45**, 1112 (1980).

[2]J. F. van der Veen, F. J. Himpsel, and D. E. Eastman, Phys. Rev. Lett. **44**, 189 (1980).

[3]P. Heimann, J. F. van der Veen, and D. E. Eastman, Solid State Commun. **38**, 595 (1981).

[4]T. Miller, E. Rosenwinkel, and T.-C. Chiang, Solid State Commun. **47**, 935 (1983); Phys. Rev. B **30**, 570 (1984).

[5]T. Miller, T. C. Hsieh, and T.-C. Chiang, Phys. Rev. B **33**, 6983 (1986).

[6]A. L. Wachs, T. Miller, and T.-C. Chiang, Phys. Rev. B **33**, 8870 (1986).

[7]T.-C. Chiang, Comments At. Mol. Phys. **13**, 299 (1983).

[8]H. C. Gatos and J. Lagowski, J. Vac. Sci. Technol. **10**, 130 (1973).

[9]L. J. Brillson, Surf. Sci. Rep. **2**, 123 (1982).

[10]J. E. Demuth, W. J. Thompson, N. J. DiNardo, and R. Imbihl, Phys. Rev. Lett. **56**, 1408 (1986).

[11]G. Margaritondo, L. J. Brillson, and N. G. Stoffel, Solid State Commun. **35**, 277 (1980); L. J. Brillson, Phys. Rev. B **18**, 2431 (1978).
[12]T. Miller, A. P. Shapiro, and T.-C. Chiang, Phys. Rev. B **31**, 7915 (1985).
[13]C. R. Brundle, J. Vac. Sci. Technol. **11**, 212 (1973).
[14]T. Miller and T.-C. Chiang, Phys. Rev. B **29**, 7034 (1984).
[15]R. Ludeke, T.-C. Chiang, and T. Miller, J. Vac. Sci. Technol. B **1**, 581 (1983).
[16]R. Ludeke, T.-C. Chiang, and D. E. Eastman, J. Vac. Sci. Technol. **21**, 599 (1982).
[17]R. Ludeke, T.-C. Chiang, and D. E. Eastman, Physica **117&118B**, 819 (1983).
[18]D. J. Chadi, Phys. Rev. Lett. **43**, 43 (1979).
[19]R. M. Tromp, R. J. Hamers, and J. E. Demuth, Phys. Rev. Lett. **55**, 1303 (1985).
[20]R. Ludeke, IBM J. Res. Dev. **22**, 304 (1978); A. Y. Cho, J. Appl. Phys. **47**, 2841 (1976); P. Drathen, W. Ranke, and K. Jacobi, Surf. Sci. **77**, L162 (1978).
[21]T.-C. Chiang, J. A. Knapp, M. Aono, and D. E. Eastman, Phys. Rev. B **21**, 3513 (1980).
[22]T.-C. Chiang (unpublished).
[23]P. H. Citrin and G. K. Wertheim, Phys. Rev. B **27**, 3176 (1983).
[24]P. Steiner and S. Hufner, Solid State Commun. **37**, 279 (1981); P. Steiner, S. Hufner, N. Martensson, and B. Johansson, *ibid.* **37**, 73 (1981).
[25]M. G. Mason, Phys. Rev. B **27**, 748 (1983).
[26]R. M. Friedman, J. Hudis, M. L. Perlman, and R. E. Watson, Phys. Rev. B **8**, 2433 (1973).
[27]T. K. Sham, M. L. Perlman, and R. E. Watson, Phys. Rev. B **19**, 539 (1979).
[28]S. M. Sze, *Physics of Semiconductor Devices*, 2nd ed. (Wiley, New York, 1981), p. 849.
[29]C. A. Mead and W. G. Spitzer, Phys. Rev. **134**, A713 (1964).
[30]R. C. Baetzold, J. Chem. Phys. **68**, 555 (1978).
[31]R. K. Swank, Phys. Rev. **153**, 844 (1976).